STUDIES ON POLYPYRROLE NANOSTRUCTURES

A dissertation submitted in partial fulfillment of the requirement for the award of the degree of

MASTER OF TECHNOLOGY
IN
POLYMER TECHNOLOGY

By

ARUNAVA PRAMANIK
Roll No. – 2K14/PTE/02

Under the esteemed guidance of

Prof. (Dr.) D. Kumar

Department of Applied Chemistry & Polymer Technology
Delhi Technological University
(FORMERLY DELHI COLLEGE OF ENGINEERING)

JULY 2016

Department of Applied Chemistry & Polymer Technology

Delhi Technological University, Delhi

(FORMERLY DELHI COLLEGE OF ENGINEERING)

CERTIFICATE

This is to certify that the dissertation entitled ***"Studies on polypyrrole nanostructures"*** *is being submitted by* ***Arunava Pramanik (2K14/PTE/02)*** *to the* ***Delhi Technological University, Delhi*** *for the degree of* ***Master of Technology*** *in* ***Polymer Technology*** *is a bonafide work carried out by him. The research reports and the results presented in this thesis have not been submitted in parts or in full to any other University or Institute for the award of any degree.*

Prof. (Dr.) D. Kumar
Ex-Head

Prof. R. C. Sharma
Head

DECLARATION

I, **ARUNAVA PRAMANIK (2K14/PTE/02)** a student of Master of Technology (POLYMER TECHNOLOGY), hereby declare that the thesis entitled "**STUDIES ON POLYPYRROLE NANOSTRUCTURES**" is an authentic record of research work done by me. This report work has not been submitted previously for the award of any degree or diploma of this university or any other university/ Institute.

Place: DTU, DELHI

Date:

ARUNAVA PRAMANIK

2K14/PTE/02

M.Tech (Polymer Technology)

ACKNOWLEDGEMENT

I wish to express my sincere gratitude to ***Dr. D. Kumar,*** Professor of Department of Applied Chemistry & Polymer Technology, Delhi Technological University, Delhi, who has graciously provided me his valuable time whenever I required his support. His counseling, supervision and suggestions were always encouraging and it motivated me to complete the project at hand. He will always be regarded as a great mentor for me.

I would like to express my profound gratitude to ***Dr. Chandra Mouli Pandey***, DST-INSPIRE Faculty, Department of Applied Chemistry & Polymer Technology, DTU. At many stages in the course of this research project I benefited from his advice, particularly when exploring new ideas. His positive outlook and confidence in my research inspired me and gives me confidence.

I would like to express my heartiest thank to faculty members, staff members, my seniors and colleagues for constant support and motivation throughout my programme. Last but not least, I thank my parents, for everything I am and will be in future. It is your unspoken prayers and affection that keep me moving forward.

ARUNAVA PRAMANIK
Roll No.: 2K14/PTE/02
Department of Applied Chemistry &
Polymer Technology
Delhi Technological University

ABSTRACT

In the present work, an attempt has been made to synthesize various nanostructures of polypyrrole (PPy) using MnO_2 as a reactive template. This approach exploits the possibility of MnO_2 morphologies and its versatility as a sacrificial template. These nanostructures have been characterized using scanning electron microscopy; Fourier transform infrared spectroscopy, thermogravimetric analysis, and X-ray diffraction techniques. Particle size analysis shows that the synthesized structure has a size of ~100 nm. These unique architectures of PPy nanostructures may provide an increased electroactive surface area that leads to rapid ion and electron transfer with excellent strain accommodation. Further, the PPy nanostructures can be properly tuned for the practical applications of these materials in electrochemical energy storage and biomedical devices etc.

Contents

List of figures Page No

List of Tables **Page No**

CHAPTER 1

INTRODUCTION & LITERATURE REVIEW

1.1 Introduction

Before 1970, polymers sound to be an insulator of electricity. They were widely used for the purpose of insulation, like in insulating wires and cables, in electronics and electrical industries, etc. The notion of human that plastics could be made for the conduct of electricity would have been observed to be absurd. They were used as insulating material and for inactive packaging. This very narrow perspective is rapidly changing as a new class of polymers known as intrinsically conducting polymers (CPs), or electroactive polymers is being discovered.

CPs have a broad range of applications because the synthetic metals as a result of they can be used as alternate for metals and semiconductors through a considerable form of electronic and electrical devices and additionally keep the mechanical properties of the traditional polymers [1]. CPs are distinctive photonic and electronic functional materials due to their high π-conjugated length, unusual conducting mechanism, and reversible redox doping/de-doping method. The features of the CPs like high thermal stability, facile synthesis, bio-compatibility, electrochemical properties, important electrical conductivity, reversibility, stability in air, switching capability between the conducting-oxidized and the insulating reduced. CPs shows numerous promising applications, in transistors, memories, sensors, artificial muscles, supercapacitors, and lithium ionic batteries [2, 3]. However, ICPs face some limitations as they are brittle, infusible and insoluble material and suffers from poor processability as a result of their highly rigid conjugated backbone structure [4]. Their mechanical strength of the CPs is poor which restricts its applications in various areas [5]. Thus there is a need to prepare CPs based on organic–inorganic hybrid materials in which CPs are used as an organic component and various transition or non-transition metal oxides as an inorganic counterpart.

In the past decade, CPs nanostructures became a rapidly growing field of research, as they show new properties associated with their nanoscale size which has significantly improved the performance of devices. CPs nanostructures have been synthesized by using various approaches, like well-controlled solution synthesis [6], soft-template methods [7], hard-template methods [8], and electrospinning technology [9]. In recent years, the low carbon economy of sustainable and renewable resources has become an excellent challenge due to global climate change and also the

decreasing availability of fossil fuels. It is currently essential to develop new, low-cost and environmentally friendly energy conversion and storage systems. Recent advances have already been created in the field of energy storage that includes rechargeable lithium ionic batteries and super-capacitors. CPs like polyaniline, polypyrrole and polythiophene have sensible electrochemical activities that make them conducting materials for pseudo-capacitors and rechargeable lithium batteries. Compared with bulk CPs, the nanostructures are expected to show improved performance in technological applications [10]. These distinctive properties arises from that nano-scale size: (i) high electrical conductivity [11]; (ii) massive specific surface area [12]; (iii) improved cycle life due to better accommodation of the strain caused by electrochemical reaction [13]; (iv) short path lengths for the transport of ions; (v) mixed conductive mechanism of each electronic and ionic conductivity, that lowers the interfacial impedance between electrolyte and electrodes; (vi) light weight and huge ratio of specific discharge power to weight. In this context, template synthesis has offered a facile, efficient and extremely manageable route for the designing and synthesis of a novel class of CPs nanostructures and composites.

Among the various CPs, polypyrrole (PPy) is one of the most successful members of the conducting polymers family due to its inherent properties, like excellent conductivity, environmental stability, redox properties, biocompatibility and so forth [14]. On the other hand, it is still challenging to fabricate any desired nanostructure of PPy. The nanostructure of PPy can be synthesized using chemical and electrochemical oxidation of pyrrole in organic solvents and in an aqueous medium which contains positive charges on the backbone. Most frequent approaches for the fabrication of various nanostructures of PPy include hard and soft template methods. However, each of these categories has its own drawbacks. The hard template method needs additional template removal treatments which can damage the original nanostructure whereas the soft template methods involve the use of doping polyanions, surfactants, etc., which raise environmental concerns.

1.2 Conducting polymer

Polymers are long chain molecules that are made up by covalent linkages of repeating units of monomers, e.g., plastics, elastomers, fibers. Polymers are considered to be insulators, but

recently electrically conducting polymers have been discovered. The requirement of polymer to be electrically conductive is that it should consist of alternating single and double bonds, i.e., conjugated double bonds.

CPs are increasingly replacing natural and inorganic materials in an application requiring excellent mechanical properties and light weight. The mechanical properties of polymers can be modified to offer durable materials with high toughness and low resistance. In the early 1990s, an important discovery in the development of CPs was the high conductivity of polysulphide nitride $(SN)_x$ [14], an inorganic polymer, which becomes superconducting at about 0.3K. This was the first polymer that was displayed to have metallic properties. In the late 1970s, many researchers focused their interests on organic conducting polymers because they believed that these materials probably might be processed by conventional plastic technology.

Polymers are insulators because the atoms in the polymer chain are covalently bonded. In this covalently bonded molecules of saturated carbon compounds, there is no scope of delocalization of valence electrons, and subsequently, neither charge carriers or path of their movements available. Since in conjugated molecules of carbon compounds, delocalization may occur through the interaction of π-bonded electrons, such molecules may be conducting. Thus it was thought that a long chain conjugated molecule, such as a polymer of acetylene, may prove to be conducting. In fact, it was proposed, purely from the theoretical consideration that appropriately substituted polyacetylene (PA) molecule would exhibit even superconducting behavior at room temperature [15]. In 1977, the high electrical conductivity of an organic polymer, doped polyacetylene was reported by H. Shirakawa in Japan, Alan G. MacDiarmid of University of Pennsylvania and A. G. Heeger, University of Califonia [16]. They discovered that partial oxidation with iodine or other reagents made polyacetylene films material with a metallic conductivity. It was suggested that plastics could indeed, under certain circumstances, be made to behave very much like metal, for which H. Shirakawa, Alan G. MacDiarmid, and A. G. Heeger was awarded the Nobel Prize in chemistry for the year 2000. The conductivity of doped polyacetylene was as high as 1000 S/cm which was greater than that of any known polymer. Polyacetylene has limited commercial application because of its processing difficulty and rapid fall in conductivity when exposed to air. Iodine doped polyacetylene is not the only conducting polymer, several other polymers have been found to exhibit conductivity on doping. Ever since

the invention of extremely conducting polyacetylene, a couple of new polymers are added to the list of the conducting polymers like polypyrrole, polyaniline, polythiophene, polyparaphenylene, polyphenylenevinylene, etc.

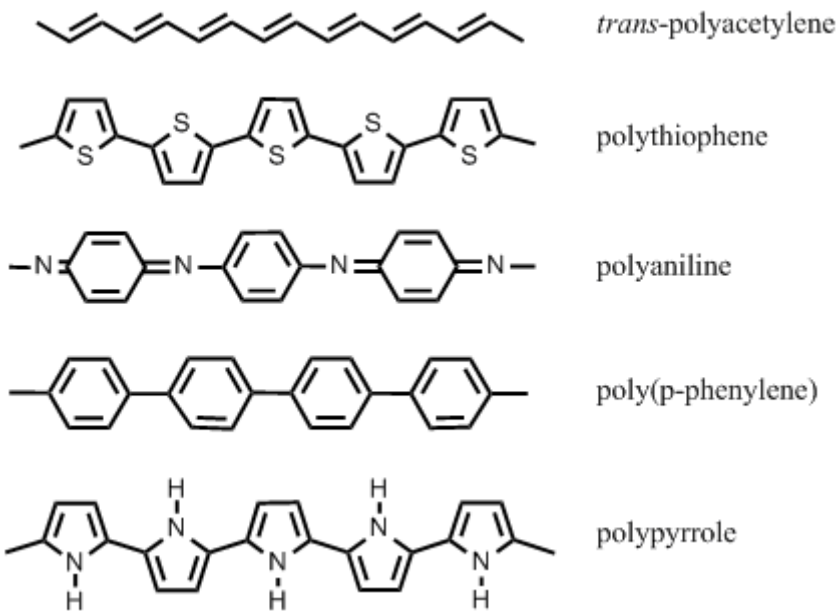

Figure 1: Some examples of conducting polymers

The most interesting aspect is that the conductivity can be made to vary over a very wide range, starting from insulator to semiconductor and to metallic, by changing the concentration of dopant. Some problems associated with trans-polyacetylene include its extreme sensitivity to oxygen and its solubility in common organic solvents. Tourbillion and Garnier prepared polythiophene by electro-chemical polymerization method [17]. It can be doped with both n type and p type dopants and the doping level of 50% can be achieved. Such a high value of dopant has been associated with the partial crystalline nature of this conducting polymer. Conducting polyparaphenylene (PPP) can be synthesized electrochemically and its chemical conductivity can be increased by some orders of magnitude on suitable doping. This polymer has also been found to unstable in air and hence cannot be used for industrial application [18].

Polypyrrole (PPy) with high conductivity (8 S/cm) can be prepared as a dense conducting film by using electro-chemical polymerization. A disadvantage is that it is not possible to produce conducting PPy with electron donating species. PPy is stable in air but it is not soluable in common organic solvent. It is however a good electrode material and a number of applications for PPy have been proposed [16]. A significant advantage over other doped polymers is the

excellent stability of doped polyphenylenevinylene (PPV) under normal atmospheric conditions and at temperatures in excess of 400 ^{o}C.

Amongst the several conducting polymers, polyaniline (PANI) has rapidly become the subject of considerable interest for physicists, chemists, and material scientists. PANI exists in several oxidation states with electrical conductivity varying from 1–10 S/cm to more than 10 S/cm. However, only one form called the emeraldine salts is electrically conducting. It can be easily synthesized by electrochemically or chemical oxidation of aniline in aqueous acidic media using common oxidant, such as ammonium peroxidisulphate. Mechanically flexible, dark blue films of conducting polyaniline also have been achieved by protonic doping of emeraldine films cast from N-methylpyrrolidone (NMP) solutions. Protonic doping accomplished either by dipping of emeraldine films in acid or passing gas, protonates the imine nitrogen atoms in the backbone of the polymer. The conducting emeraldine salt becomes the insulating emeraldine base when treated with aqueous alkali.

In the early 1980s, excitement ran high when several prototype devices based on conducting polymers, such as rechargeable batteries and current rectifying p-n junction diodes, were announced. Some predictions were made about the bright future of these new materials. One was that be the late 1980s, conducting polymers would find dozens of uses in electrical wires, polymer batteries powering devices from watches to automobiles, etc. Perhaps this expectation would have been understood, had the first conducting polymers being processable and their electronic structures better understood. However, far from behaving as plastics, the first conducting polymers were insoluble, infusible and brittle; even some polymers were unstable in air. It is important to understand the conduction mechanism and charge carriers in these exciting "Conducting Plastics" and also their application in molecular/electronics devices. Though these polymers are used in several applications, their processability and stability is the major problems which most of the polymer scientists are trying to overcome.

1.2.1 Conduction mechanism and electrical behavior in conducting polymers

Conducting polymers are a category of organic semiconductors having a negative temperature element of conduction and hence the idea of standard semiconductors was used to discuss the conductivity mechanism. A key demand for a compound to become conducting is that there

ought to be overlap of molecular orbital to permit the formation of delocalized molecular wave functions. Besides this, molecular orbital should be partly crammed, so there's a free movement of electrons throughout the lattice [19]. In band theory, the atomic orbital of every atom overlap with an equivalent orbital of neighboring atoms altogether directions to supply molecular orbital almost like those in tiny molecules. Once these orbital's area unit spaced along in a very given vary of energies, they from what sounds like continuous energy bands.

The electrical properties of standard inorganic semi-conducting materials depend on the band structure. Once the bands area unit partly crammed or empty, no conductivity happens. If the band gap is slender at temperature, thermal excitation of electrons from the valence band to conductivity band provides rise to conduction. This is often what happens in classical semiconductors. Once the band gap is too wide, thermal excitation is short to excite the electrons across the gap and solid in dielectric. The high conduction of metals is due to partially occupied bands, a partly crammed conductivity bands, a partly empty valence band or a zero band gap. So as to grasp the behavior of conducting polymers, it is essential to grasp regarding the sort of charge carriers and also the band structure.

1.2.2 Charge carriers in conducting polymers

Conducting polymers are having a peculiar behavior of charge carriers which have been explained using the idea of solutions, polarons and bipolarons. A radical cation that's partly delocalized over some polymer segment is termed a polaron. It stabilizes itself by polarizing the medium around it. When an electron is removed from the top of the valence band of a conducting polymer, a vacancy (hole or radical cation) is formed that doesn't delocalize utterly, as would be expected from classical band theory. Solely part delocalization happens, extending over a several monomeric units and affecting them to deform structurally. The energy related to this radical cation represents a destabilized bonding orbital and therefore contains a higher energy than the energy within the valence band. This rise in the energy takes place when an electron is removed from a filled bonding molecular orbital. If another electron now could be removed from the already oxidized polymer containing the polaron, two things will happen. This electron might return from either a different segment of the polymer chain, therefore making another independent polaron level, or from the primary polaron level to make a special dication,

that is termed bipolaron. Low doping levels produce to polarons, wherever higher doping levels manufacture bipolarons. Compared to polaron, bipolaron is doubly charged however spinless.

The bipolaron also has structural deformation associated with it. The two positive charge of the bipolaron are not independent, but acts as a pair, much like the copper pair in the Bardeen-Copper-Schrieffer (BCS) theory of superconductivity. Both polarons and bipolarons are mobile and can move along the polymer chain by the rearrangement of single and double bonds in the conjugated system that take place in an electric field. If many bipolaron are formed, approximately as an effect of high doping their energies can start overlapping at the edges, which creates narrow bipolaron bands in the band gap. Polyacetylene has a degenerate ground state and in polyacetylene, the bipolarons dissociate into independent cations which are spin-less and are called solitons. Solitons do not form in polymers with degenerate ground state, such as polypyrrole, polythiophene and polyphenylene. These polymers are called nondegenerate because their resonance forms not identical if they are superimposed. The conc. of charge solitons increases with doping using a suitable dopant.

1.2.3 Band gap in conducting polymer

The energy difference between the highest occupied energy band and the lowest unoccupied energy band is called the band gap or the energy band gap. The highest occupied energy band is called the valence band and the lowest unoccupied energy band is called the conduction band. Conducting polymers might be a class of polymers that would have a very low energy band gap. The energy band gap controls the optical and the electronic properties of conducting polymers. The energy band gap of many well suited conducting polymers is more than 2.0 eV. Thus for some polymers, that of poly(paraphenylene) is 2.7 eV, that of polypyrrole is 3.2 eV, that of polythiophene is 2.0-2.1 eV, that of poly(p-phenylenevinylene) is 2.4 eV, etc. Polyacetylene having the lowest energy band gap of about 1.5 – 1.7 eV [20].

Band gap energy,

$$E_g = E_g(0) - \beta_0 T$$

where, $E_g(0)$ is the energy band gap in -273^0C temperature,

β_0 is material constant which is different for different materials and

T is the ambient temperature.

Energy band gap depends on temperature. Energy band gap is inversely proportional to the temperature. If temperature is increases then energy band gap is decreases and so conductivity of the polymer increases. So, we can conclude that conductivity of polymer is proportional to the temperature.

1.2.4 Synthesis of conducting polymers

There are many methods well-known for the synthesis of conducting polymers. However, the most widely used technique is the oxidative coupling involving the oxidation of monomers to create a radical cation followed by coupling to di-cations and also the repetation results in the polymer. Electro-chemical synthesis is also rapidly becoming the preferred general methodology for preparing electrically conducting polymers due to simplicity and reproductivity. The advantage of the electro-chemical polymerization is the reaction will be carried out at temperature. By varying either the voltage or current with time, the thickness of film may be controlled. The most disadvantage of conducting polymers is instability. The subsequent are the preliminary details relating the method used for synthesis of conducting polymers.

1.2.4.1 Electrochemical polymerization

Polymers such as polypyrrole, polyaniline, polythiophene are prepared by electrochemical polymerization. In this method appropriate potential is applied to working electrode soaked in aqueous electrolytic solution containing the monomer. This method enables exact control of thickness by passing suitable electrical charge. Electro-chemical polymerization also helps in doping to enhance usefulness and also produces freestanding films. It is cost effective because film can be deposited over small area of electrode. Electrochemical polymerization of conducting polymers is generally employed by 1) Constant current or galvanstatic, 2) Constant potential or potentiostatic and 3) Potential scanning/cycling or sweeping methods. Standard electro-chemical technique which employs a divided cell containing a working electrode, a counter electrode and a reference electrode generally produces the best films. The commonly used anodes are platinum, gold, nickel, chromium, palladium, titanium and indium-tin oxide coated glass plates. Semi-conducting materials such as n-doped silicon, gallium arsenide, cadmium sulphide and semi-metal graphite are also used for the growth of polymer films.

1.2.4.2 Chemical polymerization

Chemical polymerization is the most useful method for preparing large amounts of conducting polymers, since it is performed without electrodes. Chemical polymerization is followed by the oxidation of the monomers to cation radical and their coupling to form dications and the repetition of this process generates a polymer. All the classes of conjugated polymers may be synthesized by this technique.

1.2.4.3 Chain growth polymerization

Ziglar-Natta was the first who prepare polymer by using chain growth polymerization method. He carried out extensive investigation into the direct polymerization of acetylene, and reported that bubbling of acetylene gas through a solution of a typical ziglar catalyst in hydrocarbon solvent resulted in the preparation of trans-polyacetylene as semiconductor red powder. Polyacetylene is prepared by the passage of pure dry acetylene gas over $TiCl_4/Al(C_2H_5)_3$ catalyst solution in toluene at -78 ^oC. The polymer film is obtained in the surface of the catalyst solution. The film obtained was 98% cis-polyacetylene.

CPs can be synthesized by standard chain growth polymerization method like chain growth method or step growth methods. For chain growth method catalysts like Ziglar-Natta are frequently used. Synthesis of CPs by anionic chain growth process the carbon disulfide has been used. Earlier these polymers were synthesized by heating the monomer at moderately high temperatures. Some example of the conducting polymers which have been synthesized by chain growth polymerization method using iron, copper chloride as catalysts include polypyrrole, polythiophene, etc. These conducting polymers are obtained in the form of powder.

1.2.4.4 Step polymerization

Step polymerization involves condensation reaction between two reactive groups of different molecules. For instance polyphenylene is prepared by step polymerization method. Polyphenylene sulphide is prepared by polycodensation of para-dichlorobenzene with sodium sulphide. Similarly polyvinylene sulphide and polythiophene sulphide have been prepared by polycondensation between appropriate dichloro compound and anhydrous sodium sulfide.

Photochemicals and other methods are also used for film development; however these methods are not frequently used.

The step growth polymerization proceeds usually through the condensation reaction bifunctional monomers to give a linear polymer. This polymerization is used to synthesize a polymer containing heteroatom in the backbone. Polymerization reaction is carried out either at 140 ^{o}C temperature or at 19 atm pressure.

1.2.5 Doping techniques

Doping of polymers may be carried out by the following methods.

1. Gaseous doping
2. Solution doping
3. Electrochemical doping
4. Self doping and
5. Radiation induced doping.

Of these, first three techniques are widely used because of convenience and low cost.

In the gaseous doping, polymers are exposed to the vapour of dopants under vaccum. The level of dopant concentration in the polymers may be easily controlled by the temperature, vaccum and the time of exposure.

Solution doping involves the use of solvent (toluene, acetonitrile, tetrahydrofuran, nitro-methane, etc.) in which all the products of doping are soluble.

In electrochemical doping only ionic types dopants are used as the electrolyte in polar solvents such as nitro-methane, acetonitrile, dichloromethane, tetrahydrofuran, etc.

Self doping does not require any external doping agent. In the polymer chain ionizable group, for example sulphonate group of poly[3(2-ethane sulphonate) thiophene] acts as a dopants for the polymer [21].

In radiation induced doping, high energy radiation such as gamma rays, electron beam and neutron radiation are used for the polymers. For example gamma rays irradiation in the presence of SF_6 [22] gas and neutron rays irradiation in the presence of I_2 [23] has been used for doping of polythiophene.

1.2.6 Stability of conducting polymers

1.2.6.1 Thermal stability

Thermal stability of most of the conducting polymers is poor except the heterocyclic polymers. The rate of thermal degradation is very much dependent on the environment. For example, polyacetylene degrades at room temperature in air or oxygen atmosphere but in helium atmosphere, its degradation starts in 320 ^oC [24]. Similarly, polythiophene and its derivatives are stable up to 200 to 250 ^oC in air but do not decompose up to 700^0C in inert atmosphere [25]. Nature of dopants also affects the thermal stability of polymers. For example, polypyridine doped with arylsuphonate is stable up to 80 ^oC in humid environment but when doped with BF_4 it retains its stability up to 150 ^oC [26]. Incorporation of heteroatoms having non bonding electron pairs in the conjugated chain structure is increase the thermal stability of the polymers.

1.2.6.2 Environmental stability

Conducting polymers by doping become unstable in environmental conditions. The rate of reduction in conductivity of iodine-doped polyacetylene under room temperature is higher than that of its virgin state [27]. However, in dry oxygen iodine doped polyacetylene loss its conductivity more slowly than it undoped state. Polyphenylene sulphide (PPS), which is stable in virgin state, is unstable in in the presence of moisture in doped state. But in dry air or oxygen, doped PPS is stable. Polyparaphenylene is stable in air in the presence of moisture, but it is unstable in air when doped with oxidizing dopants. Polythiophene and poly(3-methyl thiophene) are stable both in doped and undoped state in the presence of moisture or air and oxygen. The stability of these polymers is attributed to the delocalization of electrons in the chain through participation of non bonding pair of electrons of the sulphar atom.

1.2.7 Factors affecting the conductivity of conducting polymers

Various factors affecting the conductivity of polymers are described as below:

1.2.7.1 Conjugation length

One of the structural features common to all the conducting polymers is the presence of conjugation. It has been found that it is the conjugation length of the polymer chain and not its chain length which is important for its electrical conductivity. The conjugation length of a polymer chain is the average distance between two defects, which interrupt the conjugation. Evidently, chain ends are such interruption, but there are also such as $O=C-CH_2$. The effect of conjugation breaking defects on the conductivity is very drastic. Experimentally it has been found that the conductivity decreases rapidly with decreasing conjugation length. For example, if the conjugation length is decreased from its pristine value 100Å to about 10Å in the case of trans-PA chains, the conductivity decreases by 8 orders of magnitude.

Mathematically,

$$R = \rho L/A$$

or, $\rho = RA/L$

or, $1/\sigma = RA/L$

or, $\sigma \propto L$

Where, R is resistance value of material,

L is the conjugation length,

A is the area of cross-section of material,

ρ is the resistivity of the material and

σ is the conductivity of the material.

1.2.7.2 Temperature

In order to understand the effect of temperature on the conductivity of polymers, first of all it is reasonable to define two conductivity regimes. The high conductivity regimes with conductivity 1000 S/cm and the modest and low conductivity regimes with conductivity 100 S/cm. Majority of conducting polymer belongs to the modest and low conductivity regime. The temperature

difference is different in two conductivity regimes. In both conductivity regimes, the conductivity decreases when the temperature is lowered implying hereby that the temperature coefficient for a synthetic metal is different from that of metal in which the conductivity in cooling the metal. In modest and low conductivity regime, the conductivity vanishes as the temperature approaches to zero whereas in high conductivity system the conductivity is remains finite. Further, the conductivity dependence of the conductivity also varies with the level of doping. For example, for low-doped PA samples, the temperature dependence of the conductivity is very drastic. As the doping level increases, the dependence of conductivity on doping becomes less and less and for highly doped samples, the conductivity is found to be nearly temperature dependent.

1.2.7.3 Doping level

The conductivity of the conjugated polymers can be increased by increase in the doping level of these polymers. The doping level of the polymer is determined by the dopant concentration expressed in mol%. The enhancement of electrical conductivity primarily depends on the chemical reactivity of the dopant with the polymer. The same dopant cannot be effective for the different polymers. For example iodine enhances the conductivity of polyacetylene by 10-12 orders of magnitude but it fails to dope polyphenylene sulfide or polyparaphenylene because of its weak oxidizing ability.

1.2.8. Applications of conducting polymers

There are two main groups of applications for these polymers. The first group utilizes their conductivity as its main property. The second group utilizes electro-activity. The extended π-systems of conjugated polymer are highly susceptible to chemical or electrochemical oxidation or reduction. By controlling the oxidation and reduction, it is possible to precisely control their electrical and optical properties. Since these reactions are often reversible, it is possible to systematically control these properties with a great deal of precision. The two main groups of applications are as follows:

1. Electrostatic materials, conductive adhesives, electromagnetic shilding, printed circuit boards, artificial nurves, antistatic clothing, piezoceramics, active electronic and aircraft structures.
2. Molecular electronics, electrical displays, biochemical and thermal sensors, rechargeable batteries and electrolytes, drug release systems, ion exchange membranes, optical computers, electromechanical actuators and small structures.

1.3 Polypyrrole

Polypyrrole (PPy) was first discovered in 1963, at that time it was called pyrrole black. PPy is one type of organic polymers which are synthesized by using pyrrole monomer. PPy is generally synthesized by using chemical or electrochemical polymerization method. Chemical polymerization method involves mixing a strong oxidizing agent (in general $FeCl_3$) with a monomer solution and is used when large quantities of materials are required [28]. Electrochemical polymerization method is mainly preferred for research purposes because of the simplicity of the technique, to control over material thickness, geometry and location, the ability for doping during polymerization, the wide variety of available dopant ions and the production of good quality films [29].

1.3.1 Synthesis

Weiss and coworkers reported polypyrrole in 1963. These workers described the pyrolysis of tetraiodopyrrole to produce highly conductive materials [30]. Most commonly PPy is prepared by oxidation of pyrrole monomer, which can be achieved by using ferric chloride in methanol:

$$n\ C_4H_4NH + 2\ FeCl_3 \rightarrow (C_4H_2NH)_n + 2\ FeCl_2 + 2\ HCl$$

Polymerization is consideration to occur by the formation of π-radical cation $C_4H_4NH^+$. This electrophile attacks of C-2 carbon of an un-oxidized molecule of pyrrole to provide a dimeric cation $(C_4H_4NH)_2]^{2+}$. This process repeats itself many times.

Conductive forms of the PPy are prepared by using oxidation (p-doping) of the polymer:

$$(C_4H_2NH)_n + x\ FeCl_3 \rightarrow (C_4H_2NH)_nCl_x + x\ FeCl_2$$

The polymerization and p-doping can be affected electrochemically. The resultant conductive polymers are peeled off of the anode. Cyclic voltammetry and chronocoulometry methods can be used for the electrochemical synthesis of PPy [31].

1.3.2 Properties of PPy

PPy films darken in air due to some oxidation. Doped PPy films are blue or black depending on the degree of polymerization and thickness of the films. They are amorphous in nature and showing only weak diffraction. Undoped or doped PPy films are insoluable in many solvents but they are swellable. Doping makes the polymer brittle. PPy is stable in air upto a temperature 150 ^{o}C at which temperature the dopant start to evolve [32]. PPy is an insulator, however its oxidized derivatives are sensible electrical conductors. The conductivity of the material depends on the conditions and reagents utilized in the oxidation. Conductivities range from 2 to 100 S/cm.

1.3.3 Applications of PPy

PPY can often be used as biosensors, gas sensors, microactuators, antielectrostatic coatings, solid electrolytic capacitor, electrochromic windows and displays, packaging, polymeric batteries, electronic devices and functional membranes etc. PPy coatings have an excellent thermal stability and are good candidate for use in carbon composites. To further enhance the properties of PPy, metal oxide nanoparticles are used.

1.4 Metal oxide nanoparticles

Presently, the group of the most important nanomaterials includes simple metal oxides such as manganese oxide (MnO_2), zinc oxide (ZnO), titanium oxide (TiO_2), magnesium oxide (MgO), copper oxide (CuO), aluminium oxide (Al_2O_3) and iron oxide (Fe_3O_4, Fe_2O_3). Metal oxides NPs are finding increasing application in a wide range of fields and represent about one-third of the consumer products nanotechnology market. These materials are used as pigments in paints (TiO_2), as sunscreens and cosmetics (TiO_2, ZnO), as antimicrobial agents (MgO, CuO), in industrial operations (Al_2O_3, MnO_2) and for medical purposes (Al_2O_3, Fe_3O_4, Fe_2O_3). Aluminium nanomaterials act as drug delivery systems, by encapsulating the drugs the drugs to increase

solubility for evading clearance mechanisms and allowing the site-specific targeting of drugs to cells.

1.4.1 Manganese oxide (MnO_2)

Manganese oxide is an inorganic compound which is blackish or brown in colour. This solid occurs naturally because the mineral pyrolusite, which is the main ore of manganese (Mn) and a component of Mn nodules. The principal use for MnO_2 is in dry-cell batteries, like the alkaline battery and the zinc-carbon battery. MnO_2 is additionally used as a pigment and as a precursor to alternative Mn compounds, like $KMnO_4$. It is used as a chemical agent in organic synthesis, as an example, for the oxidation of allylic alcohols. MnO_2 in the polymorph will incorporate a variety of atoms in the "tunnels" or "channels" between the magnesium oxide octahedral. There is considerable interest in α-MnO_2 as a possible cathode for lithium ion batteries.

1.5 MnO_2 PPy composites

The combination of PPy and manganese dioxide will give synergetic effect. For example, Dong et al prepared manganese oxide (MnO_2)/doped PPy by chemical oxidative polymerization [33]. It is observed that the dispersed MnO_2 adhered to PPy chains increased the specific surface area of the nanocomposite and retarded the structural deterioration of PPy backbones during charge-discharge cycling process. Due to the synergic effect between MnO_2 core and PPy shell, the MnO_2 at PPy coaxial nanotubes possess better rater capability, larger specific capacitance and good capacitance retention. Bahloul prepared PPy covered MnO_2 by electrodepositing PPy on MnO_2 particles and found that the presence of PPy improves the electrochemical performance of the composite material electrode and increases the specific capacitance [34]. It is evident that the MnO_2/PPy composites own a better capacitance performance than pure MnO_2 or pure PPy.

1.6 Aims and Objectives

This project deals with the preparation of PPy nanostructures using MnO_2 template. A systematic methodology highlighting the progress of the proposed work involves following steps:

- Preparation of MnO_2 template (i.e., nanorods and nanowires)
- Characterization of MnO_2 template
- Preparation of PPy nanostructures using MnO_2 template (i.e., nanotubes and nanofibers)
- Characterization of PPy nanostructures
- Analysis of results

CHAPTER 2

METHODOLOGY &

CHARACTERIZATION TECHNIQUES

2.1 Introduction

This section deals with the synthesis and characterization of MnO_2 nanorods, MnO_2 nanowires, PPy and PPy nanostructures. The details of their preparation and characterization are described.

2.2 Materials and apparatus used:

Potassium permanganate ($KMnO_4$) (CDH), concentrated hydrochloric acid (HCl) and distilled water were used for the synthesis of MnO_2 nanorods. Manganese sulphate monohydrate purified ($MnSO_4,H_2O$) (CDH), ammonium persulfate ($(NH_4)_2S_2O_8$) (CDH), ammonium ferrous sulfate ($(NH_4)_2SO_4,FeSO_4,6H_2O$) (CDH) and distilled water were used for the synthesis of MnO_2 nanowires. MnO_2 templates, distilled water, conc. HCl, potassium dichromate ($K_2Cr_2O_7$) (CDH) and pyrrole monomer (Sisco Research Laboratories Pvt. Ltd.) were used for the preparation of PPy nanostructures. Ferric chloride ($FeCl_3$) (CDH), distilled water and pyrrole monomer were used for the preparation of PPy. Ethanol (Changshu Yangyuan Chemical, China) and distilled water was used for washing. Magnetic stirrer, ultrasonicator bath, teflon-lined stainless steel autoclave with a cavity of 100 ml and oven were used in this study.

2.3 Synthesis

2.3.1 Synthesis of MnO_2 nanorods

MnO_2 nanorods were prepared using hydrothermal method. In brief, 0.025 M (4.0 gm) of potassium permanganate was dissolved into 50 ml of distilled water. Then 1.5 ml of concentrated HCl (37%) was added in the solution with stirring for 2 h. Then the solution was transferred to a teflon-lined stainless steel autoclave (capacity of 100 ml). Then the autoclave was kept in an oven at 140 ^oC temperature for 10 h. After reaction, the product was washed with distilled water and ethanol a number of times and dried in an oven overnight.

2.3.2 Synthesis of MnO_2 nanowires

MnO_2 nanowires have been prepared by using a simple co-precipitation method. 0.1 M manganese sulphate monohydrate purified and 0.1 M ammonium persulfate were mixed into 100 ml distilled water with stirring for 1 h. Where $MnSO_4$ and $(NH_4)_2S_2O_8$ were used as sources of

manganese and oxidizing agent, respectively. MnO_2 nanowires were prepared by adding 0.05 M ammonium ferrous sulfate in the solution with stirring for 1 h. Then the precursor was maintained at 80 ^oC for 1 h. Then the solution was kept in room temperature for a night. The product was cleaned sequentially with water and ethanol and finally dried in an oven at 80 ^oC overnight.

2.3.3 Synthesis of PPy nanostructures

Two different PPy nanostructures have been synthesized by using the corresponding two morphologies of MnO_2 as sacrificial templates. Typically, 100 mg of MnO_2 nanorods or nanofibres were dispersed into 30 mL of distilled water with stirring for 30 min followed by bath sonication for 30 min, in which 1 M HCl (37%) was added. Then 200 µl of pyrrole monomer and 0.1 g of $K_2Cr_2O_7$ were added with stirring for 30 min followed by another 30 min of bath sonication. Later, the solution was stirred for 4 h and maintained at room temperature for 16 h. The product obtained was washed repetitively with distilled water and ethanol for several times and then vacuum dried at 60 ^oC for 8 h. Following the same approach, two different nanostructures of PPy; nanotubes and nanofibers have been synthesized which are consequently named PPy-NTs and PPy-NFs respectively.

2.3.4 Synthesis of PPy

PPy was prepared by using chemical polymerization method. 0.2 M pyrrole monomer and 1 gm ferric chloride were added in to 100 ml distilled water with stirring for 6 h using magnetic stirrer. Then the product obtained was filtered, washed repetitively with distilled water and ethanol for several times and then dried at 60 ^oC for overnight.

2.4 Characterization techniques

2.4.1 Scanning electron microscopy (SEM)

A scanning microscope (SEM) is a type of electron microscope which produces images of the samples by scanning it using a focused beam of electrons. The electrons are interacts with the atoms in the sample and produces various signals that contain information regarding the sample's surface topography and composition. The electron beam is usually scanned in an exceedingly formation scan pattern and therefore the beam's position is combined with the detected signal to provide a picture. SEM can be able to do resolution higher than 1 nm. Specimens will be observed in high vacuum, in low vacuum, in wet conditions and at a wide range of cryogenic or elevated temperatures. A pictorial view of scanning electron microscope is shown in Fig. 2.1.

Figure 2.1: A pictorial view of SEM HITACHI, model no. S-3700N with EDX with X-ray

2.4.2 X-ray diffraction (XRD)

X-ray powder diffraction (XRD) is a high-speed analytical technique mostly used for phase determination of a crystalline material and can also be used to get information about unit cell dimensions. The analyzed material is finely ground, homogenized, and average bulk composition is calculated. X-ray diffraction is based on constructive interference of monochromatic X-rays with a crystalline sample. These X-rays are produced by a cathode ray tube, which is then filtered to generate monochromatic radiation, collimated to condense, and directed to the sample. The interaction of the incident rays with the sample cause constructive interference and a diffracted ray is produced, when conditions satisfy Bragg's Law ($n\lambda=2d \sin \theta$). A pictorial view of XRD spectrophotometer is shown in Fig. 2.2 below.

Figure 2.2: A pictorial view of XRD spectrophotometer

2.4.3. Fourier transform infrared spectroscopy (FTIR)

FTIR reckons on the fact that most of the molecules absorb light in the infra-red range of the electromagnetic spectrum. This absorption corresponds particularly to the bonds of the molecule. The frequency range is calculated as wave numbers over the range of 4000 – 400 cm^{-1}. The background emission spectrum of the infra-red source is recorded, followed by the emission spectrum of the infra-red source with the sample in place. The ratio of the sample emission spectrum to the background emission spectrum is directly related to the sample's absorption spectrum. The resultant absorption spectrum due to the bond natural vibrational frequencies shows the presence of different chemical bonds and functional groups in the sample. FTIR is specifically useful for identification of organic molecular groups and compounds because of functional groups, side chains and cross-links involve will have characteristic vibrational frequencies in the infra-red range. A pictorial view of FTIR spectrophotometer is shown in Fig. 2.3 below.

Figure 2.3: A pictorial view of FTIR spectrophotometer

4.4 Thermogravimetric analysis (TGA)

Thermogravimetric analysis (TGA) relies on the measurement of mass loss of material as a function of temperature. In this analytical technique when a material is heated at a uniform rate or kept at a constant temperature a continuous graph of mass change versus temperature is obtained. The measurement is generally carried out in air or in an inert atmosphere of nitrogen, helium or argon, and the mass loss is recorded against increasing temperature. A plot of mass change versus temperature (T) is considered as the thermogravimetric curve (TG curve) or TGA thermogram. A pictorial view of TGA instrument is given in Fig. 2.4 below.

Figure 2.4: A pictoral view of TGA (Model Q50)

2.4.3 Particle Size Analysis

Particle size analyzer is an innovative particle characterization system. It provides accurate and reliable particle size analysis for a various range of applications by utilizing the verified theory of Mie-compensation for spherical particles and also the proprietary principle of modified Mie calculations for non-spherical particles. It is optimized for materials below 1 µm delivering unsurpassed resolution. It measures particle size from 0.01 to 3000 µm. It consists of tri–laser, blue/red, multi-detector and multi-angle optical system. By utilizing the blue lasers the resolution of low-end measurements will increase to dramatically improve the accuracy of measurements below one micrometer. A pictorial view of particle size analyzer is given in Fig. 2.5 below.

Figure 2.5: A pictorial view of particle size analyzer

CHAPTER 3

RESULTS & DISCUSSION

3.1 FTIR analysis

Fourier transform infrared spectroscopy is one of the most powerful analytical techniques, which offers the chemical identification.

3.1.1 FTIR spectra of MnO_2 nanorods

The FTIR spectra of hydrothermally synthesized MnO_2 nanorods are shown in figure 3.1. The broad band at 3438 cm^{-1} indicates O–H stretching in water molecules, and the weak band at 1633 cm^{-1} may be due to bending vibration of O–H groups in the adsorbed water molecules. The characteristic peaks at 1384, 1007 and 935 cm^{-1} correspond to the coordination of Mn by the O–H. The characteristic peak at 506 cm^{-1} is deemed as the main characteristic absorption band of birnessite, which corresponds to the Mn-O stretching modes of the octahedral layers in the birnessite. We therefore conclude that the products are MnO_2 template (nanorods) which is found in good agreement with the EDX analysis.

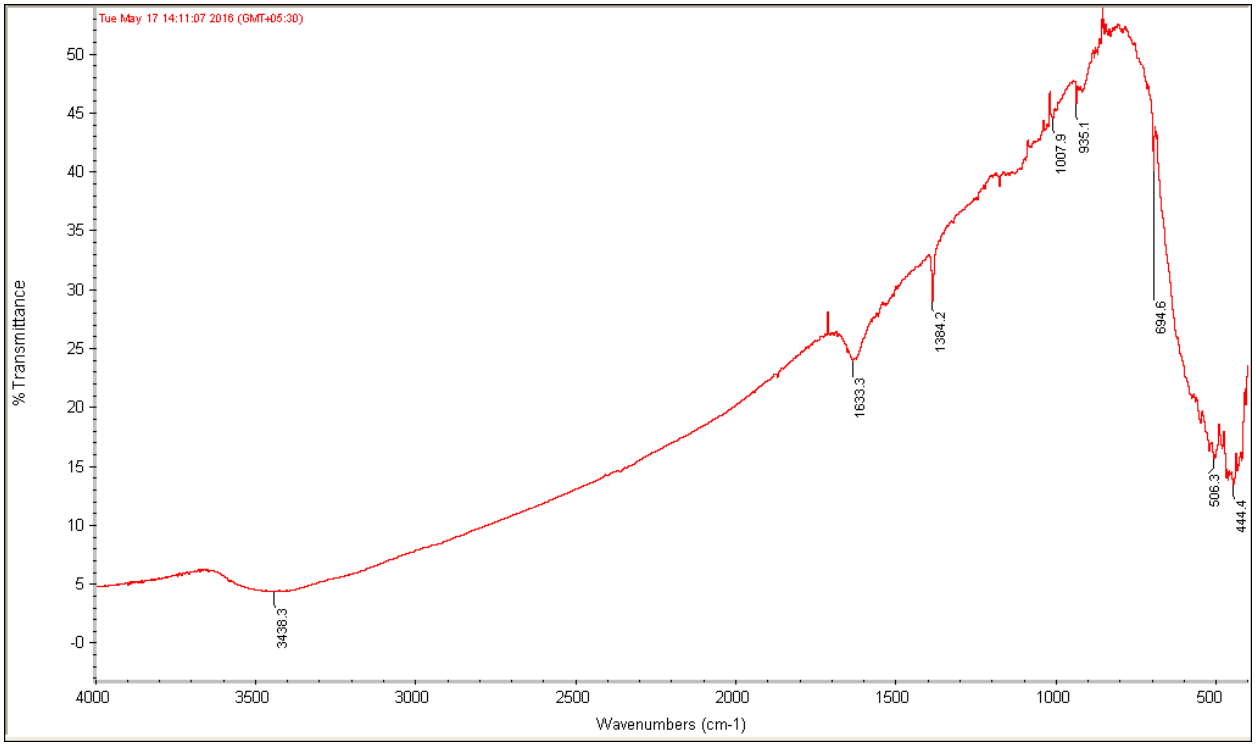

Figure 3.1: FTIR spectra of MnO_2 nanorods

3.1.2 FTIR spectra of MnO_2 nanowires

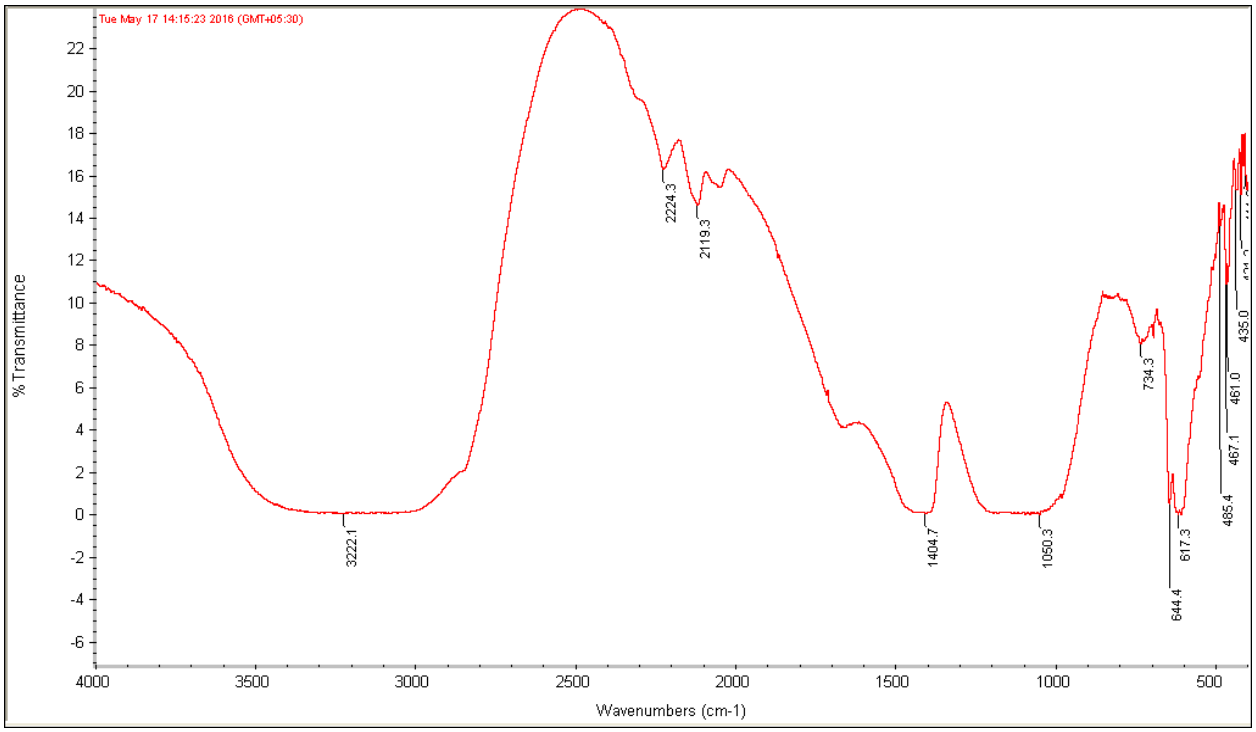

Figure 3.2: FTIR spectra of MnO_2 nanowires

To investigate molecular orientation of MnO_2 nanowires, we conducted FT-IR spectra analysis. As shown in above figure 3.2, the broad band at 3222 cm^{-1} indicates O–H stretching in water molecules, and the weak band at 2224 and 2119 cm^{-1} may be due to bending vibration of O–H groups in the adsorbed water molecules. The characteristic peaks at 1404, 1050 cm^{-1} correspond to NH_4^+, SO_4^{2-} respectively. The characteristic peak at 734 cm^{-1} corresponds to the coordination of Mn by the O–H. The characteristic peak at 644 and 617 cm^{-1} may corresponds to the Mn-O stretching modes of the octahedral layers in the birnessite. We therefore conclude that the products are MnO_2 template (nanowires) which is also found in good agreement with the EDX analysis.

3.1.3 FTIR spectra of PPy

The FTIR spectra obtained for PPy (shown in figure 3.3) show the presence of characteristic absorption band at 1541 cm^{-1} due to the C=C stretching of pyrrole ring. The characteristic peaks are at 1378 cm^{-1} may be due to the C-N stretching vibration in the ring, 1167 cm^{-1} due to the C-

H in-plane deformation, 1046 cm^{-1} due to the N-H in-plane deformation and 913 cm^{-1} may be due to the C-H out-of-plane deformation.

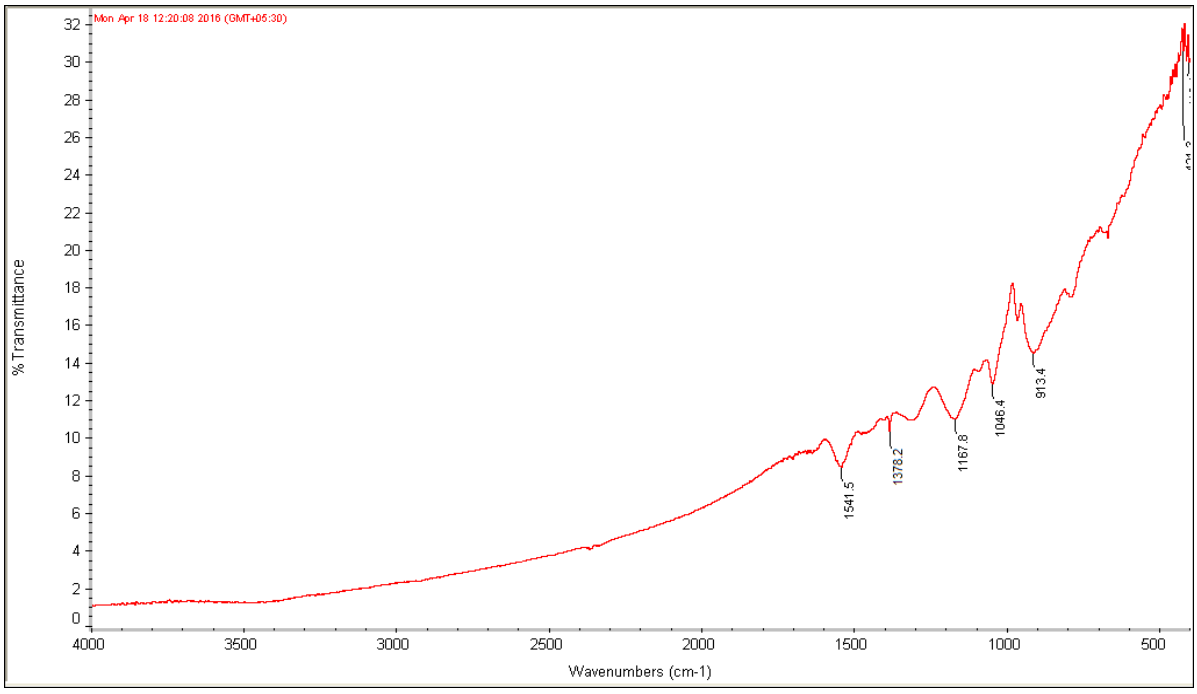

Figure 3.3: FTIR spectra of PPy

3.1.4 FTIR spectra of PPy nanotubes

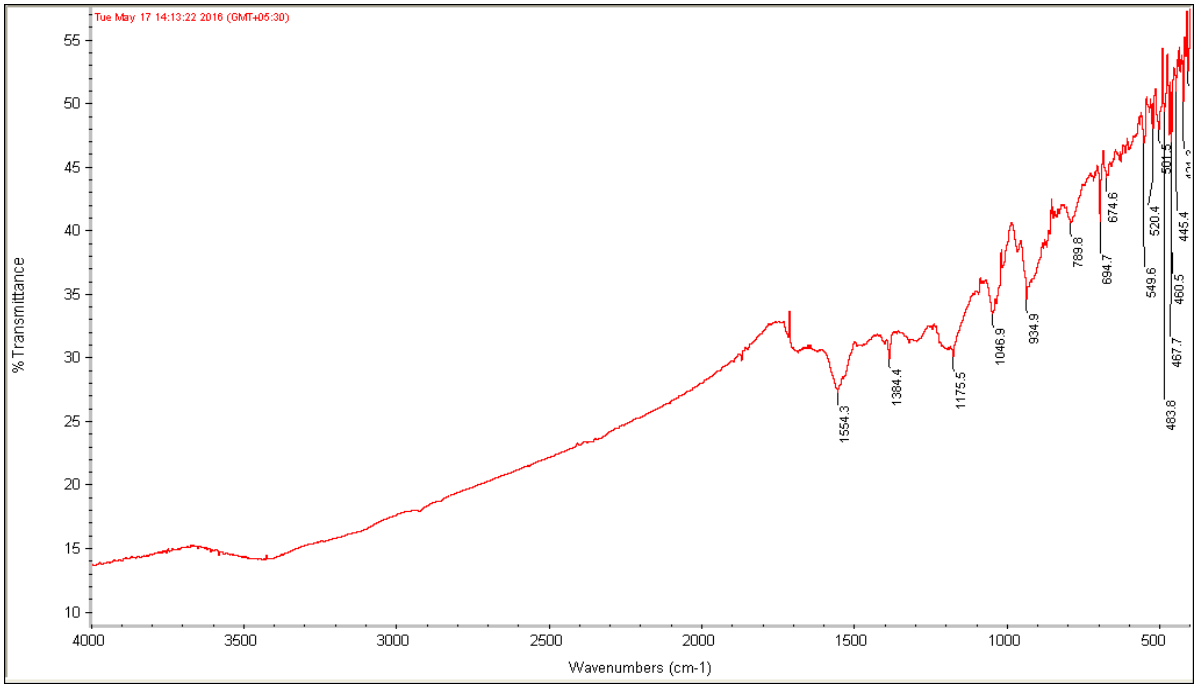

Figure 3.4: FTIR spectra of PPy nanotubes

The FTIR spectra recorded for PPy nanotubes (shown in figure 3.4) show the presence of characteristic absorption band at 1554 cm^{-1} due to the C=C stretching of pyrrole ring. The characteristic peaks found at 1384 cm^{-1} may be due to the C-N stretching vibration in the ring, 1175 cm^{-1} due to the C-H in-plane deformation, 1046 cm^{-1} due to the N-H in-plane deformation, 934 cm^{-1} may be due to the C-H out-of-plane deformation and 789 cm^{-1} due to the C-H out-of-plane ring deformation.

3.1.5 FTIR spectra of PPy nanofibers

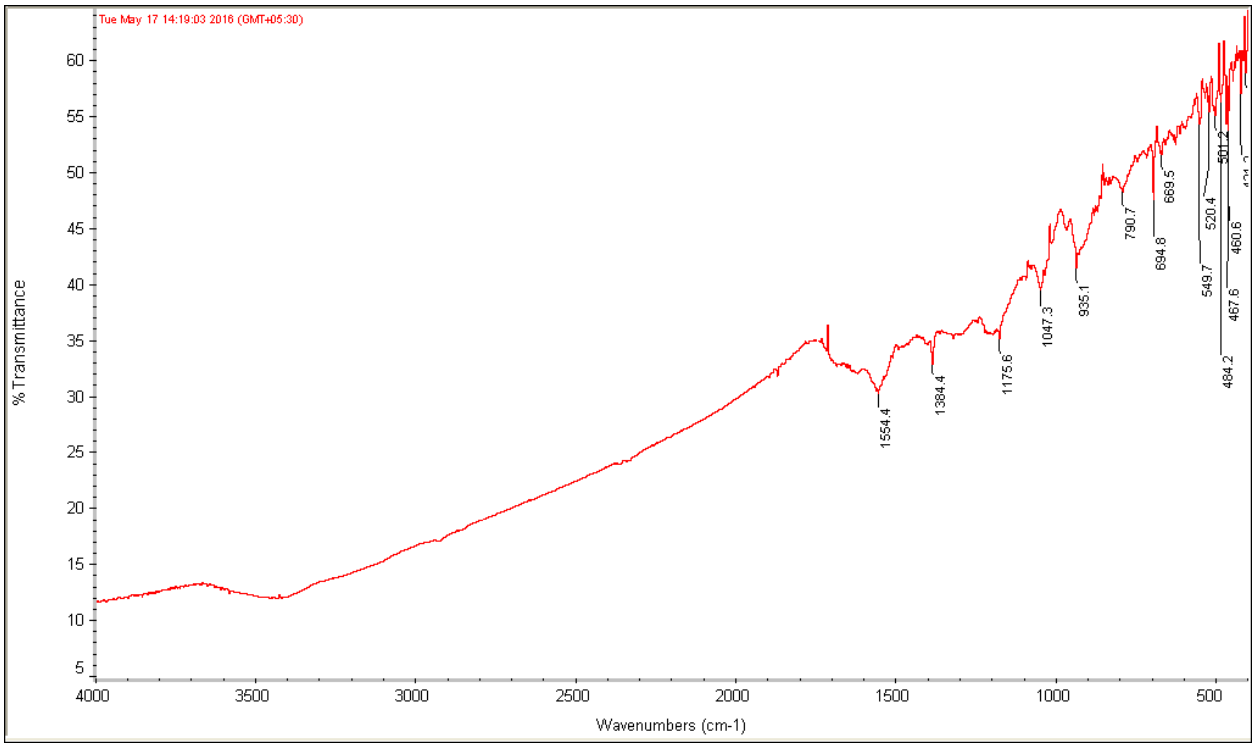

Figure 3.5: FTIR spectra of PPy nanofibers

The FTIR spectra recorded for PPy nanofibers are shown in the above figure 3.5. It shows the presence of characteristic absorption band at 1554 cm^{-1} due to the C=C stretching of pyrrole ring. The characteristic peaks found at 1384 cm^{-1} may be due to the C-N stretching vibration in the ring, 1175 cm^{-1} due to the C-H in-plane deformation, 1047 cm^{-1} due to N-H in-plane deformation, 905 cm^{-1} due to the C-H out-of-plane deformation and 790 cm^{-1} due to C-H out-of-plane ring deformation.

3.2 SEM Studies

The morphological behaviour of different samples was investigated by using scanning electron microscopy technique and SEM micrographs of these samples are presented in Fig. 3.6 as given below.

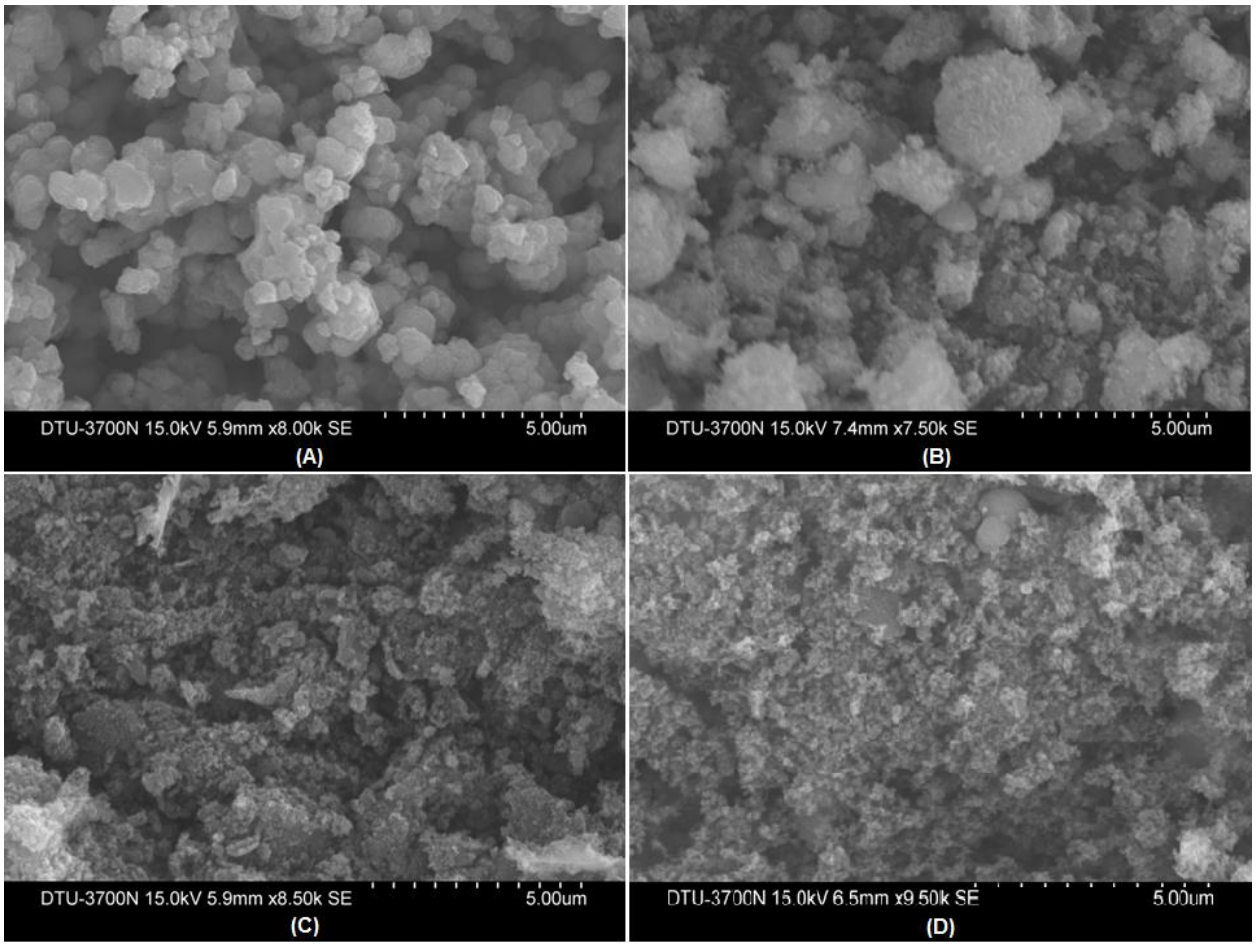

Figure 3.6: SEM images of nanostructures of MnO_2 (A) nanorods and (B) nanowires with PPy (C) nanotubes and (D) nanofibers

Figure 3.6 (A–B) shows two completely different morphologies of MnO_2, namely, nanorods and nanowires, that were used as sacrificial templates to arrange nanotubes and nanofibers of PPy, respectively as shown in figure 3.6 (C-D). It is interesting to notice that even after a dense deposition of PPy, all two original nanostructures of MnO_2 were successfully preserved by the polymer. The PPy nanostructures formation mechanism are often rationalized as follows and it is schematically shown in figure 3.7. Initially, pyrrole monomer is adsorbable on the outer surface

of solid MnO_2 nanostructures yielding an adsorbate-covered solid-liquid interface and then the redox reaction between pyrrole monomer and MnO_2 takes place at the interface in presence of HCl, which ends up in the formation of oligo and polymeric species (PPy) of pyrrole following an instant dissolution of MnO_2. The interfacial polymerisation of PPy continues till the entire removal of MnO_2 and also the nanostructured PPy is finally obtained. The oxidation potential of MnO_2 is 1.23 V, which is enough for the polymerization of pyrrole monomer on the surface of the MnO_2 templates, since the oxidation potential of pyrrole monomer is about 0.7 V. As the redox reactions proceed, the rigid templates are sacrificed whereas pyrrole monomer is polymerized surrounding the templates and that results in the formation of the aforementioned PPy nanostructures [35].

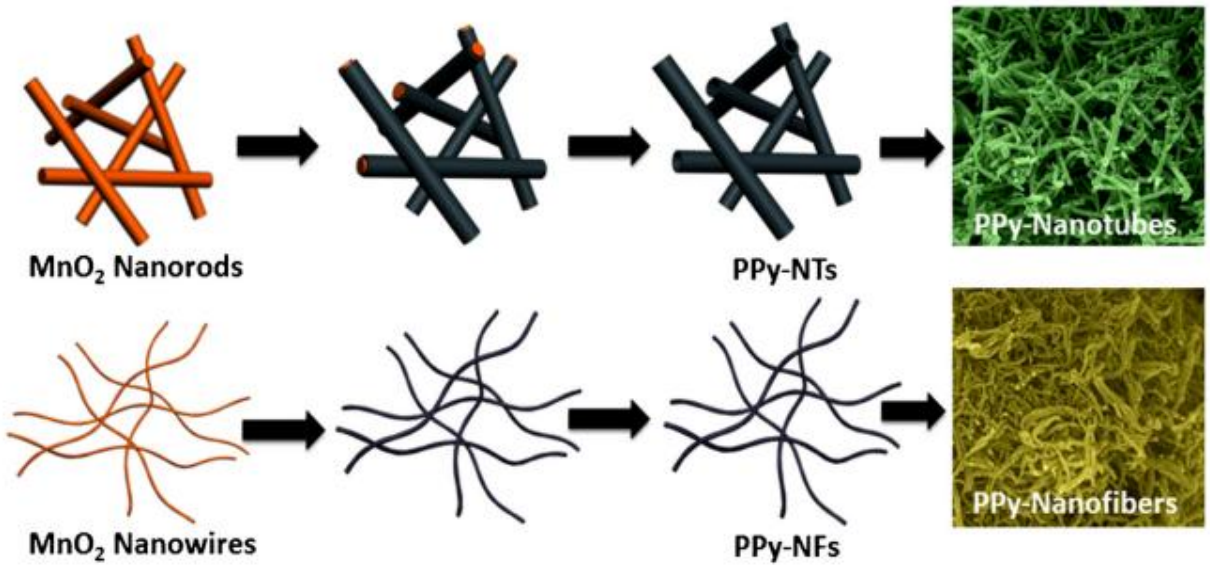

Figure 3.7: Schematic illustration of steps involved in growth of PPy nanostructures by the tunable morphology of MnO_2 as reactive templates.

3.3 EDX analysis

3.3.1 EDX report of MnO_2 nanorods

The chemical composition of MnO_2 nanorods was extracted from energy dispersive X-ray spectrum (Access Voltage: 15.0 kV, Take off Angle: 43.4 deg.). From figure 3.8, it can be seen clearly that many peaks are present due to Mn which are found at access voltage 0.5, 6 and 6.5 keV, a peak present due to O is found at access voltage 0.5 keV and some other peaks present

due to K and Cl are found at access voltage 2.5, 3, 3.25 and 3.5 keV, respectively. The atomic percentage of Mn and O elements present in the MnO_2 nanorods are found to be 64.88%, 24.34%, respectively. The EDX spectra of MnO_2 nanorods are given in the following figure 3.8.

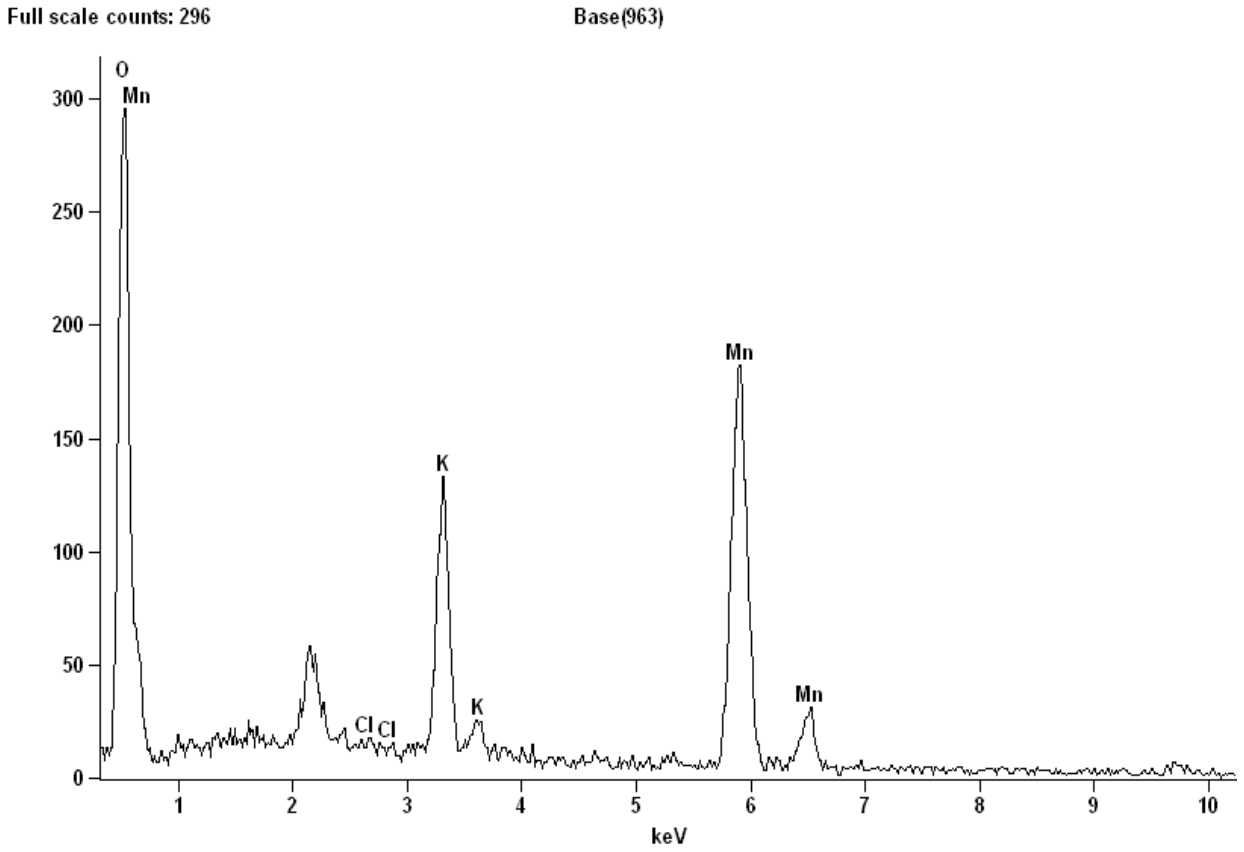

Figure 3.8: EDX spectra of MnO_2 nanorods

3.1 Table 1: Quantitative results for MnO_2 nanorods

Element Line	*Net Counts*	*Int. Cps/nA*	*Weight %*	*Weight % Error*	*Atom %*	*Atom % Error*	*Formula*	*Standard Name*
O K	2411	---	24.34	+/- 0.61	51.08	+/- 1.27	O	
Cl K	51	---	0.29	+/- 0.12	0.28	+/- 0.11	Cl	
Cl L	0	---	---	---	---	---		
K K	1527	---	10.48	+/- 0.47	9.00	+/- 0.41	K	
K L	0	---	---	---	---	---		
Mn K	2991	---	64.88	+/- 2.08	39.65	+/- 1.27	Mn	
Mn L	649	---	---	---	---	---		
Total			100.00		100.00			

3.3.2 EDX report of MnO_2 nanowires

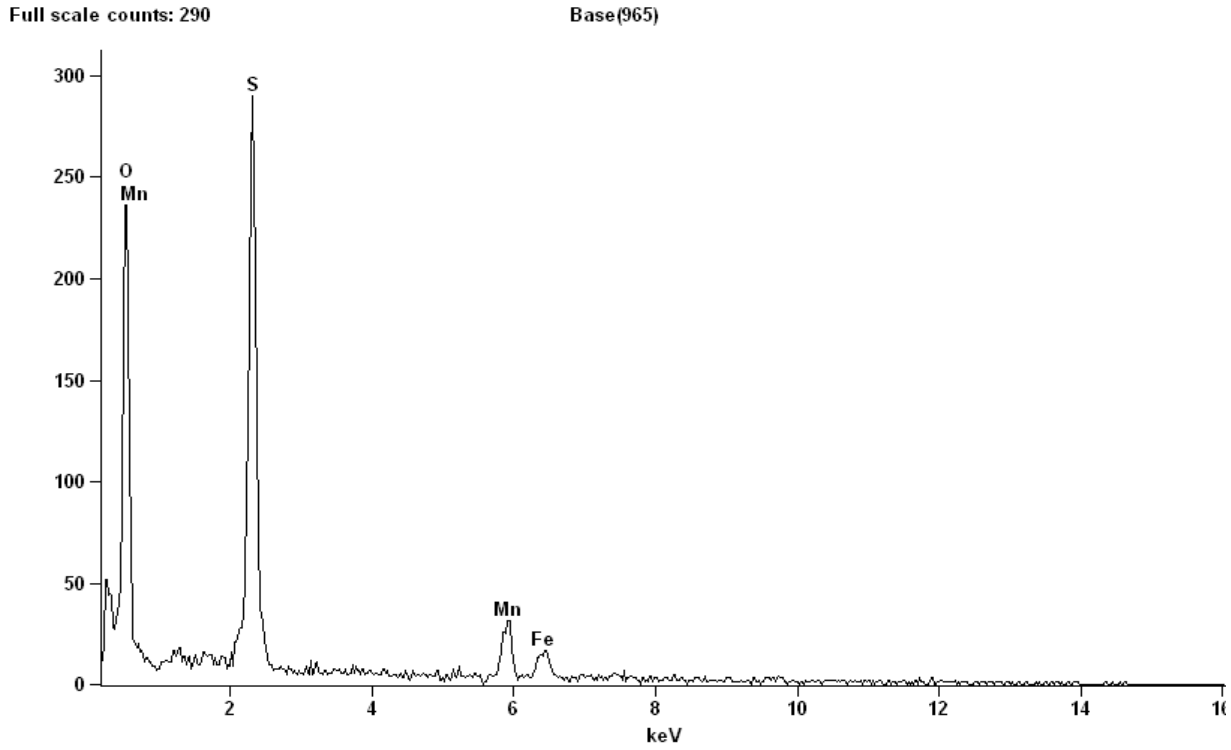

Figure 3.9: EDX spectra of MnO_2 nanowires

From the above EDX spectra, it is clear that the two peaks present due to Mn are found at access voltage 0.5 and 6 keV, a peak present due to O is found at access voltage 0.5 keV and two peaks present due to S and Fe are found at access voltage 2.5 and 6.5 keV, respectively. The atomic percentage of Mn and O elements present in the MnO_2 nanowires are 19.7%, 39.63%, respectively which is shown below in Table 2.

3.2 Table 2: Quantitative results for MnO_2 nanowires

Element Line	*Net Counts*	*Int. Cps/nA*	*Weight %*	*Weight % Error*	*Atom %*	*Atom % Error*	*Formula*	*Standard Name*
O K	1696	---	39.63	+/- 1.22	62.50	+/- 1.92	O	
S K	3171	---	30.06	+/- 0.80	23.66	+/- 0.63	S	
S L	4976	---	---	---	---	---		
Mn K	422	---	19.70	+/- 1.45	9.05	+/- 0.66	Mn	
Mn L	22	---	---	---	---	---		
Fe K	202	---	10.62	+/- 1.42	4.80	+/- 0.64	Fe	
Fe L	26	---	---	---	---	---		
Total			100.00		100.00			

3.4 XRD analysis

The X-ray diffraction (XRD) is most generally used technique for knowing the crystallinity of the material. It's used to measure the average spacing's between layers or rows of atoms, verify the orientation of a single crystal or gain. The XRD pattern obtained for as synthesized PPy nanostructures by Hummer's methodology. The XRD pattern of PPy nanostructures clearly shows the optical phenomenon peak at $2\Theta=26^0$, that represents PPy is amorphous in nature. The XRD pattern of PPy nanotubes and PPy nanofibers is presented in Fig. 3.10.

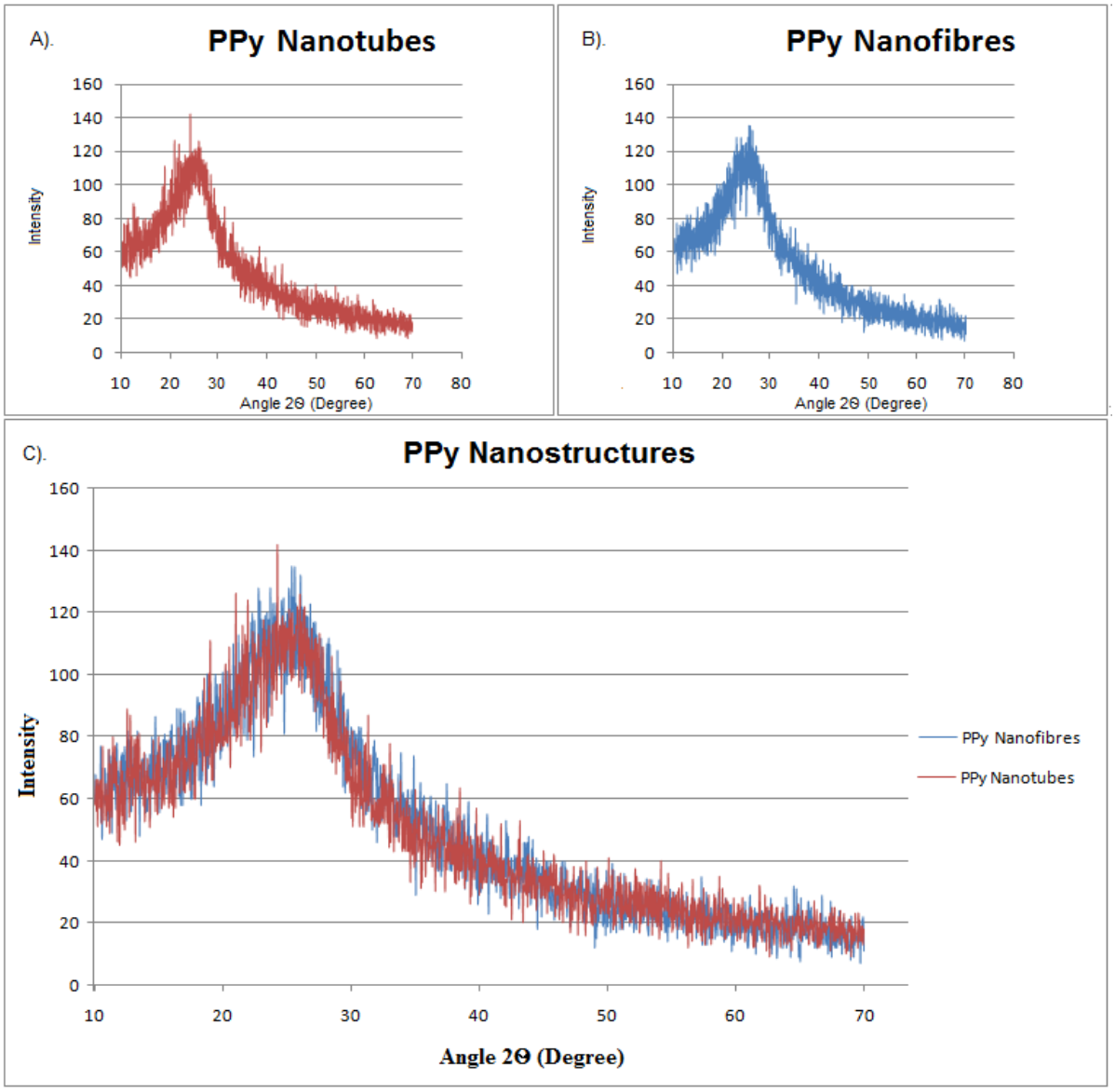

Figure 3.10: XRD pattern of PPy nanotubes and PPy nanofibers

3.5 TGA analysis

The TGA thermograms of PPy nanostructures (i.e., nanotubes and nanofibres) are shown in Fig. 3.11 given below. The TGA thermograms reveal that as the temperature increases from room temperature to 600 ^{o}C, there is a continuous weight loss of polymer. It is also noticed that as the temperature increases, % weight loss occurs at a constant rate. In case of PPy nanotubes, 10% weight loss occurs at 100 ^{o}C but in PPy nanofibres only 6% weight loss occurs due to the moisture elimination. In case of PPy nanofibers, % weight loss is greater as compared to PPy nanotubes at 600 ^{o}C.

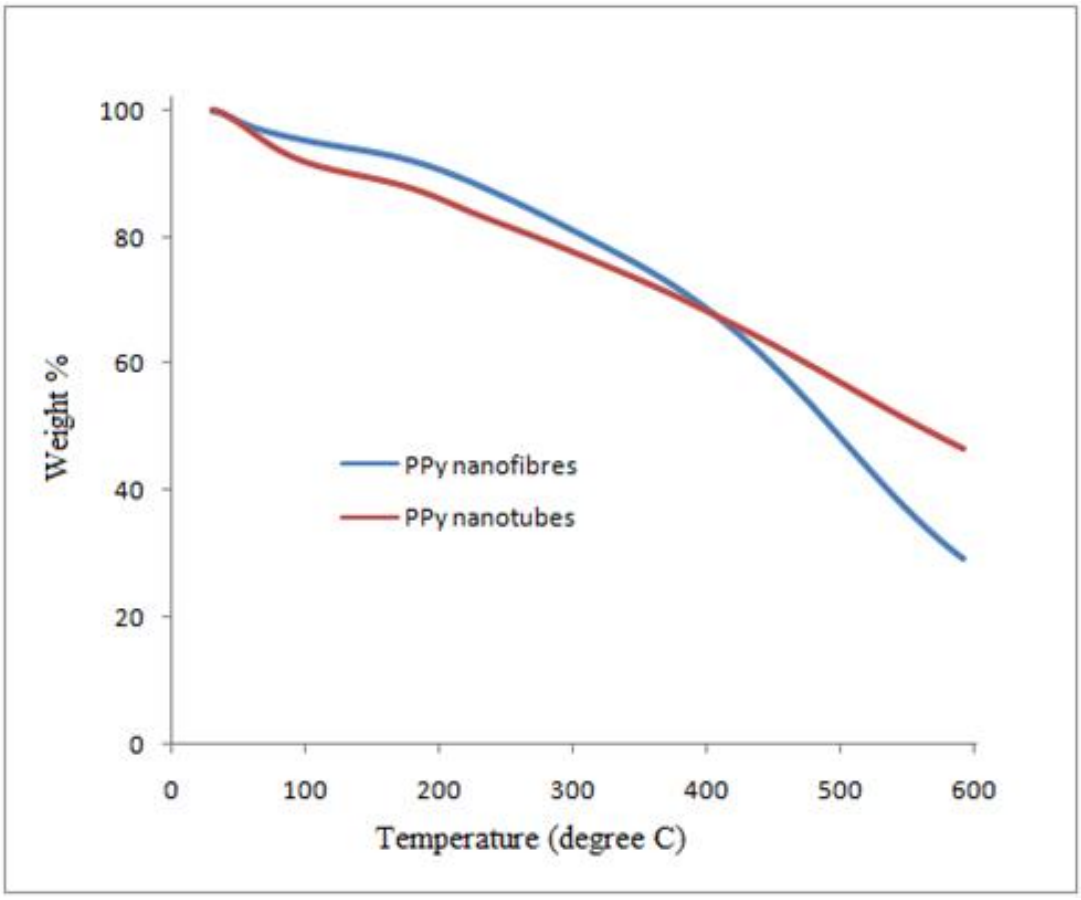

Figure 3.11: TGA thermograms of PPy nanostructures

3.5 Particle size analysis

The diameter size of the majority of the prepared PPy nanostructures samples is found in the range of 328 to 50 nm, as shown in the figure 3.12 and 3.13 while some PPy nanostructures are found in the micrometer range and some below 50 nm range.

10.6.0

Bluewave

- Particle Size Analysis -

-

-

Data Acquired: 06/24/2016 - 14:11

Calculated: 06/24/2016 - 14:11

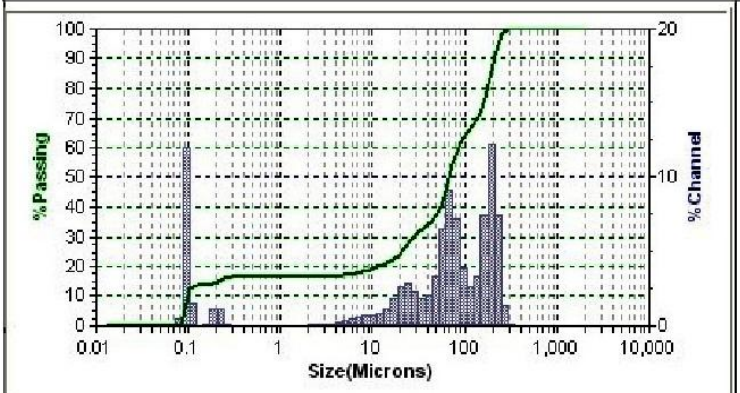

Summary

Data	Value
MV(um):	89.34
MN(um):	0.0960
MA(um):	0.622
CS:	9.65
SD:	94.71
Mz:	86.05
σ1:	81.52
Ski:	0.339
Kg:	0.646

Percentiles

%Tile	Size(um)
10.00	0.0980
20.00	11.60
30.00	27.76
40.00	54.73
50.00	68.25
60.00	84.26
70.00	139.6
80.00	179.3
90.00	206.2
95.00	225.6

Size Percent

Size(um)	%Tile

Size(um)	%Chan	% Pass	Size(um)	%Chan	% Pass
2000	0.00	100.00	5.50	0.33	17.38
1674	0.00	100.00	4.62	0.22	17.05
1408	0.00	100.00	3.89	0.15	16.83
1184	0.00	100.00	3.27	0.12	16.68
995.5	0.00	100.00	2.750	0.09	16.56
837.1	0.00	100.00	2.312	0.06	16.47
703.9	0.00	100.00	1.944	0.00	16.41
591.9	0.00	100.00	1.635	0.00	16.41
497.8	0.00	100.00	1.375	0.00	16.41
418.6	0.01	100.00	1.156	0.00	16.41
352.0	0.11	99.99	0.972	0.00	16.41
296.0	1.42	99.88	0.817	0.00	16.41
248.9	7.43	98.46	0.687	0.00	16.41
209.3	12.25	91.03	0.578	0.00	16.41
176.0	7.38	78.78	0.486	0.00	16.41
148.0	3.37	71.40	0.409	0.00	16.41
124.4	2.61	68.03	0.344	0.00	16.41
104.6	3.92	65.42	0.2890	0.15	16.41
87.99	7.20	61.50	0.2430	1.12	16.26
73.99	9.13	54.30	0.2040	1.18	15.14
62.22	6.55	45.17	0.1720	0.12	13.96
52.32	3.36	38.62	0.1450	0.00	13.84
44.00	2.00	35.26	0.1220	1.46	13.84
37.00	1.83	33.26	0.1020	11.95	12.38
31.11	2.27	31.43	0.0860	0.43	0.43
26.16	2.88	29.16	0.0720	0.00	0.00
22.00	2.67	26.28	0.0610	0.00	0.00
18.50	1.87	23.61	0.0510	0.00	0.00
15.55	1.16	21.74	0.0430	0.00	0.00
13.08	0.81	20.58	0.0360	0.00	0.00
11.00	0.71	19.77	0.0300	0.00	0.00
9.25	0.68	19.06	0.02550	0.00	0.00
7.78	0.57	18.38	0.02150	0.00	0.00
6.54	0.43	17.81	0.01810	0.00	0.00

Peaks

Dia(nm)	Vol%	Width
186.4	34.6	77.67
66.29	34.0	35.72
18.92	15.0	17.24
0.2040	2.6	0.05
0.0950	13.8	0.01

[redacted]

SOP Name: ARUNAVA(*)

Distribution:	Volume	Run Time:	10 Sec	Fluid:	CURRENTCARRIER		
Progression:	Standard	Run#:	Avg of 3	Fluid Ref Index:	1.333	Loading Factor:	0.1099
Up Edge(um):	2000	Particle:	PPY	Above Residual:	0	Trans. L1:L2:	0.976:0.804
Low Edge(um):	0.0107	Transparency:	Transparent	Below Residual:	0	RMS Residual:	0.791%
Residuals:	Disabled	Part. Ref. Index:	1.73			Flow:	70%
#Channels:	70	Particle Shape:	Spherical	Cell ID:	0098	Usonic Power:	N/A
Analysis Mode:	BLUEWAVE			Multi Run Delay:	0 Min.	Usonic Time:	N/A
Filter:	Disabled	DB Record:	253	Recalc Status:	Original	Serial Number:	S5133
Analysis Gain:	Default(2)	Database:	C:\Program Files\Microtrac FLEX 10.6.0\Databases\DTU.MDB				

Figure 3.12: Particle size analysis of PPy nanotubes

10.6.0

Bluewave

- Particle Size Analysis -

-

-

Data Acquired: 06/24/2016 - 14:17

Calculated: 06/24/2016 - 14:17

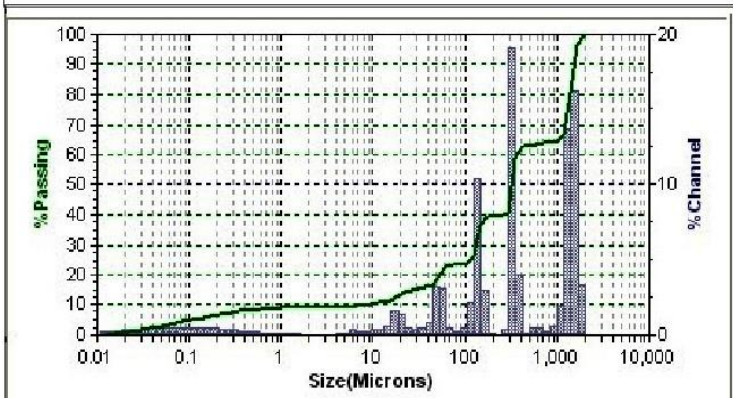

Summary

Data	Value
MV(um):	624.7
MN(um):	0.01820
MA(um):	0.586
CS:	10.25
SD:	708.3
Mz:	607.3
σ1:	602.2
Ski:	0.601
Kg:	0.554

Percentiles

%Tile	Size(um)
10.00	7.83
20.00	52.90
30.00	133.0
40.00	295.4
50.00	324.9
60.00	359.1
70.00	1250
80.00	1401
90.00	1544
95.00	1637

Size Percent

Size(um)	%Tile

Size(um)	%Chan	% Pass	Size(um)	%Chan	% Pass
2000	3.34	100.00	5.50	0.15	9.41
1674	16.20	96.66	4.62	0.06	9.26
1408	13.73	80.46	3.89	0.03	9.20
1184	1.93	66.73	3.27	0.02	9.17
995.5	0.55	64.80	2.750	0.02	9.15
837.1	0.24	64.25	2.312	0.02	9.13
703.9	0.42	64.01	1.944	0.03	9.11
591.9	0.45	63.59	1.635	0.06	9.08
497.8	0.09	63.14	1.375	0.07	9.02
418.6	3.98	63.05	1.156	0.09	8.95
352.0	19.06	59.07	0.972	0.11	8.86
296.0	0.29	40.01	0.817	0.14	8.75
248.9	0.03	39.72	0.687	0.16	8.61
209.3	0.12	39.69	0.578	0.20	8.45
176.0	2.96	39.57	0.486	0.23	8.25
148.0	10.42	36.61	0.409	0.27	8.02
124.4	2.16	26.19	0.344	0.31	7.75
104.6	0.50	24.03	0.2890	0.34	7.44
87.99	0.18	23.53	0.2430	0.38	7.10
73.99	0.46	23.35	0.2040	0.41	6.72
62.22	3.12	22.89	0.1720	0.44	6.31
52.32	3.20	19.77	0.1450	0.46	5.87
44.00	0.79	16.57	0.1220	0.48	5.41
37.00	0.48	15.78	0.1020	0.49	4.93
31.11	0.38	15.30	0.0860	0.50	4.44
26.16	0.49	14.92	0.0720	0.49	3.94
22.00	1.33	14.43	0.0610	0.48	3.45
18.50	1.57	13.10	0.0510	0.46	2.97
15.55	0.60	11.53	0.0430	0.44	2.51
13.08	0.31	10.93	0.0360	0.40	2.07
11.00	0.37	10.62	0.0300	0.37	1.67
9.25	0.26	10.25	0.02550	0.33	1.30
7.78	0.28	9.99	0.02150	0.30	0.97
6.54	0.30	9.71	0.01810	0.26	0.67

Peaks

Dia(nm)	Vol%	Width
1423	37.0	385.30
328.3	23.5	46.65
136.0	16.2	26.58
50.19	8.9	20.07
13.98	6.7	18.14
0.0710	7.7	0.16

-

SOP Name: ARUNAVA(*)

Distribution:	Volume	Run Time:	10 Sec	Fluid:	CURRENTCARRIER		
Progression:	Standard	Run#:	Avg of 3	Fluid Ref Index:	1.333	Loading Factor:	0.1057
Up Edge(um):	2000	Particle:	PPY	Above Residual:	0	Trans. L1:L2:	0.982:0.798
Low Edge(um):	0.0107	Transparency:	Transparent	Below Residual:	0	RMS Residual:	0.990%
Residuals:	Disabled	Part. Ref. Index:	1.73			Flow:	70 %
#Channels:	70	Particle Shape:	Spherical	Cell ID:	0098	Usonic Power:	N/A
Analysis Mode:	BLUEWAVE			Multi Run Delay:	0 Min.	Usonic Time:	N/A
Filter:	Disabled	DB Record:	259	Recalc Status:	Original	Serial Number:	S5133
Analysis Gain:	Default(2)	Database:	C:\Program Files\Microtrac FLEX 10.6.0\Databases\DTU.MDB				

Figure 3.13: Particle size analysis of PPy nanofibers

CHAPTER 4

CONCLUSION & FUTURE WORK

4.1 Conclusion

In summary, we can conclude that the different morphologies of polypyrrole have been successfully synthesized by using a metal oxide (MnO_2) as a template. The morphological analysis carried out by using SEM clearly shows the formation of PPy nanostructures. The sizes of these nanostructures are found mainly in the range of 50 to 100 nm. From FTIR and EDX spectra of MnO_2 templates, we can say that the characteristic peaks are present due to MnO_2, so samples may be MnO_2 template. We can conclude from FTIR spectra of PPy nanostructures that the characteristic peaks are present due to PPy and from XRD spectra it is inferred that the material is amorphous in nature, and based on the data it ensures the material formed as PPy nanostructures. The FTIR spectra of MnO_2 templates and PPy nanostructure reveal that there are no MnO_2 templates present in PPy nanostructures as characteristic peaks are not matching in both the cases. These results demonstrate the advantage of the PPy nanostructures for the design of conducting electrodes that are easy to fabricate, cost effective, and highly reproducible.

4.2 Future work

In future other metal oxide based template synthesis of the conducting polymers will be accomplished. The electrochemical properties of these nanostructures will also be studied. The formed PPy nanostructures will be deposited using electrochemical methods for possible biosensor applications.

References

1. V.K. Gade, D.J. Shirale, P.D. Gaikwad, K.P. Kakde, P.A. Savale, H.J. Kharat, B.H. Pawar, M.D. Shirsat, Int. J. Electrochem. Sci. 2 (2007) 270–277.
2. A. Kassim, H.N.M.E. Mahmud, L.M. Yee, N. Hanipah, Pac. J. Sci. Technol. 7 (2) (2008) 105.
3. H. Zengin, B. Erkan, Polym. Adv. Technol. 21 (2010) 216–223.
4. J. Jiang, L. Ai, L. Li, J. Phys. Chem. B 113 (2009) 1376–1380.
5. A. Bhattacharaya, D.C. Mukherjee, J.M. Gohil, Y. Kumar, S. Kundu, Desalination 225 (2008) 366–372.
6. Huang, J.X.; Kaner, R.B. Nanofiber formation in the chemical polymerization of aniline: A mechanistic study. Angew. Chem.: Int. Edit. 2004, 43, 5817-5821.
7. Wan, M.X. A template-free method towards conducting polymer nanostructures. Adv. Mater. 2008, 20, 2926-2932.
8. Pan, L.J.; Pu, L.; Shi, Y.; Song, S.Y.; Xu, Z.; Zhang, R.; Zheng, Y.D. Synthesis of polyaniline nanotubes with a reactive template of manganese oxide. Adv. Mater. 2007, 19, 461-464.
9. Yu, J.H.; Fridrikh, S.V.; Rutledge, G.C. Production of submicrometer diameter fibers by twofluid electrospinning. Adv. Mater. 2004, 16, 1562-1566.
10. Wu, C.G.; Bein, T. Conducting polyaniline filaments in a mesoporous channel host. Science 1994, 264, 1757-1759.
11. Penner, R.M.; Martin, C.R. Microporous membrane-modified electrodes for preparation of chemical microstructures on electrode surfaces. J. Electrochem. Soc. 1987, 134, C504-C504.
12. Pei, Q.B.; Inganas, O. Electrochemical applications of the bending beam method .1. masstransport and volume changes in polypyrrole during redox. J. Phys. Chem. 1992, 96, 10507-10514.
13. F. Yan, G. Xue, F. Wan, A Flexible Giant Magnetoresistance Sensor Prepared Completely by Electrochemical Synthesis, J. Mater. Chem. 12 (2002) 2606–2608.
14. V.V. Walatka. M.M. Labe and J.H.Perlstein., Phys.Rev.Lett.31 (1973) 1139.
15. W.A.Little. Phy. Rev., 134A (1964) 1416; Sci.Amer.212 (1965) 21.
16. H. hirakawa, E.J.Louis, A.G. MacDiarmid, C.K. Chiang and A.G. Heeger, J.Chem.Soc. Chem. Commun. (1977)578.
17. G.Tourillon and F. Garnier, J.Electroanal. Chem, 135 (1982) 173.

18. D.M. Ivory, G.G. Miller, J.M. Sowa, L.W. Shacklette, Chance abd R.H. Baughman. J.Chem. Phy., 71 (1979) 1506
19. D. Bloor and B. Movagher., IEEE Procedings. 130 (5) (1983) 225.
20. V.S.Shishodia, Application of poly(2-Ethyl Aniline) in urea biosensor, Applied Chemistry Department, DTU, (2005) p9
21. A.O. Patil, Y. Ikenoue, N. Colaneri, J. Chen, F.Wudl and A.J. Heeger., Synth. Met.20 (1987) 151.
22. K. Yoshino, S. Hayashi, K. Kaneto, J. Okube, T. Moriya, T. Matsuyama, H. Yamaoka, Mol. Cryst. Liq. Cryst. 121 (1985) 255.
23. S. Hayashi, S. Takeda, K, Yoshino and T. Matsuyama., Synth. Met. 18 (1987) 591
24. J.C.W. Chien, P.C. Uden and J.L. Fan., J. Polym. Sci. Polym. Chem. Edn. 20 (1982) 2159.
25. G. Tourillon and F. Garnier, J. Electrochem. Soc. 190 (1983) 2042.
26. H. Munstedt, H. Naaarmann and G. Kohler, Mol. Cryst. Liq. Cryst. Edn. 20 (1982) 2159.
27. H. Keiss, G. Meyer, D. Baeriswyl and G. Harbeke, J. Electron Mater 9 (1990) 763.
28. Armes 1987; Duchet et al. 1998.
29. Kumar & Sharma 1998; Inzelt et al. 2000.
30. McNeill, R.; Siudak, R.; Wardlaw, J. H.; Weiss, D. E. (1963). "Electronic Conduction in Polymers. The Chemical Structure of Polypyrrole". Aust. J. Chem. 16: 1056–75.
31. Sharifi-Viand, Ahmad. "Determination of fractal rough surface of polypyrrole film: AFM and electrochemical analysis". Synthetic metals 191 (2014) 104–112.
32. "Polypyrrole: a conducting polymer; its synthesis, properties and applications". Russ. Chem. Rev. 66 (1997) 443–457.
33. Liyang Yuan, Chuanyun Wan, Liangliang Zhao, Int. J. Electrochem. Sci., 10 (2015) 9456 – 9465.
34. A. Bahloul, B. Nessark, E. Briot, H. Groult, , A. Mauger, K. Zaghib, C.M. Julien, Journal of Power Sources 240 (2013) 267–272.
35. Deepak P. Dubal, Zahilia Caban-Huertas, Rudolf Holze and Pedro Gomez-Romero, Electrochimica Acta 191 (2016) 346–354.